Sustainable Environment Research 27 (2017) 32–40

Contents lists available at ScienceDirect

Sustainable Environment Research

journal homepage: www.journals.elsevier.com/sustainable-environment-research/

Original Research Article

Biosorption mechanism of Methylene Blue from aqueous solution onto White Pine (*Pinus durangensis*) sawdust: Effect of operating conditions

Jacob J. Salazar-Rabago [a], Roberto Leyva-Ramos [a, *], Jose Rivera-Utrilla [b], Raul Ocampo-Perez [a], Felipe J. Cerino-Cordova [c]

[a] Center for Research and Graduate Studies, Universidad Autónoma de San Luis Potosi, San Luis Potosí 78210, Mexico
[b] Department of Inorganic Chemistry, Universidad de Granada, Granada 18071, Spain
[c] Department of Chemical Engineering, Universidad Autónoma de Nuevo León, San Nicolás de los Garza 66455, Mexico

ARTICLE INFO

Article history:
Received 20 July 2016
Received in revised form
25 September 2016
Accepted 4 November 2016
Available online 24 November 2016

Keywords:
Biosorption
Chemisorption
Electrostatic attraction
Mechanism
Methylene Blue
White Pine
Wood sawdust

ABSTRACT

In this work, the biosorption mechanism of the cationic dye Methylene Blue (MB) on natural White Pine sawdust (NS) (*Pinus durangensis*) was investigated. Likewise, the surface charge distribution of NS was determined, and its point of zero charge was found to be 4.3. Besides, the capacity of the NS for adsorbing MB was increased 1.7, 2.0 and 4.6 times when the pH was raised from 3 to 4.25, 3 to 7 and 3 to 10, respectively. This behavior was attributed to the electrostatic attraction between the negatively charged surface of NS and the cationic species MB^+. The adsorption capacity increased with increased temperature because the adsorption was an endothermic process. The adsorption capacity was drastically reduced by increasing the ionic strength of the solution corroborating with the fact that the electrostatic attractions played a crucial role in the adsorption of MB on NS. It was also shown that the MB was chemisorbed because the adsorption was not reversible. The predominant adsorption mechanisms were the electrostatic attraction and chemisorption and not ion exchange.

1. Introduction

The presence of pollutants in surface and underground water resources as well as in wastewaters can seriously affect the ecosystems and human health. Among these pollutants are dyes, which can contaminate water resources due to wastewater discharges from textile, leather, food processing, dyeing, cosmetics, paper, and dye manufacturing industries [1]. The presence of dyes in water poses a significant hazard to human health since many of them are toxic, can cause allergies and irritation to the skin and the intestinal walls, and are mutagenic and carcinogenic [2].

Several separation methods have been applied for the removal of dyes from aqueous solutions. Recently, advanced oxidation processes (AOPs) based upon UV radiation have been investigated for the degradation of dyes in water solutions [3–9]. However, the main disadvantage of the AOPs was that the mineralization percentages were usually small, even though the degradation percentages of the dyes were nearly 100%. Thus, the formation of unknown intermediates with lesser or greater toxicity than the original dyes [10] can hinder the application of these AOPs.

The removal of dyes has been successfully carried out by physicochemical processes such as separation by membranes, coagulation–flocculation, adsorption and ultrasonic assisted adsorption [11–16]. The advantages of adsorption over other processes are easiness of operation, low-cost and a large number of adsorbents [2]. Various types of adsorbents have been applied for the removal of dyes including clays, zeolites, polymeric membranes, xerogels, titanium oxide nanotubes, carbon nanotubes, graphene, activated carbon and activated carbon modified by supporting ZnS:Cu nanoparticles [13,15–23]. It is well documented that the activated carbon presents the highest adsorption capacity towards dyes in aqueous solution due to the chemical nature of its surface and textural properties [2,24,25]. However, its

* Corresponding author.
E-mail address: rlr@uaslp.mx (R. Leyva-Ramos).
Peer review under responsibility of Chinese Institute of Environmental Engineering.

http://dx.doi.org/10.1016/j.serj.2016.11.009

high cost and difficult regeneration have motivated the research and development of low-cost novel adsorbents for the efficient removal of dyes from aqueous solution.

Very different biowastes have been applied as biosorbents for the removal of dyes from aqueous solutions. Some of these biowastes are bark, yellow passion fruit and mandarin peels, peanut shells, rice husks, orange and banana peels, leaves from the poplar tree, cotton, corncobs, alfalfa, bagasse, corn pericarp, agave bagasse and wood sawdust [11,12,26–33]. All these biowastes are widely available and have no economic value.

Wood sawdust is a byproduct with several practical uses, but its accumulation in soils is a serious pollution problem since sawdust can cause diseases such as asthma, allergies, chronic bronchitis and other respiratory problems [34]. Ferrero [11] and Hamdaoui [12] showed that the wood sawdust is a promising low-cost material for the treatment of polluted water containing cationic dyes since it has a high adsorption capacity compared with other agroindustrial wastes. However, it has been shown that the adsorption capacity of sawdust is significantly dependent on the species of wood. Ferrero [11] investigated the adsorption of Methylene Blue (MB), which is considered a cationic dye model, on wood sawdust from walnut, cherry, oak and pine at a solution pH between 3 and 4, and found that the adsorption capacities were 45, 38, 29 and 28 mg g^{-1}, respectively. Hamdaoui [12] studied the adsorption of MB on sawdust from natural Cedar and reported that the uptake of MB biosorbed was 142 mg g^{-1} at pH = 7 and T = 20 °C. Additionally, the experimental adsorption equilibrium data were successfully represented by the Langmuir isotherm.

In the technical literature, there is scientific controversy over the adsorption mechanism of cationic dyes on wood sawdust. Parab et al. [35] concluded that the biosorption of MB on wood sawdust was mainly controlled by chemisorption; however, Batzias and Sidiras [36] reported that ion exchange was the primary biosorption mechanism of dyes because of the chemical character of the sawdust. A literature review showed that the mechanism controlling the biosorption of MB on wood sawdust had not been advanced.

The objective of this study is to elucidate the biosorption mechanism of MB on White Pine sawdust (*Pinus durangensis*). The elucidation of the biosorption mechanism was conducted by determining the adsorption equilibrium at different pH, temperature and ionic strength, and studying the reversibility of biosorption. The biosorption mechanism is of great interest since it will enable understanding the dependence of the biosorption capacity on the operating conditions and improving the removal of MB by adsorption on sawdust.

2. Materials and methods

2.1. Natural sawdust

The natural sawdust (NS) used in this work was from White Pine (*P. durangensis*), which is a common pine species harvested in Mexico [37]. The NS was washed with deionized water and then dried in an electric oven at 80 °C for 24 h. The NS was milled, sieved to an average particle of 0.63 mm and stored in a plastic container.

2.2. Physicochemical properties of MB

The MB was used as a cationic dye model and was supplied by Sigma–Aldrich. Some of its physicochemical properties are Molecular weight = 319.9 g mol^{-1}, pK_a = 3.8, solubility in water of 43.6 × 10^3 mg L^{-1} at 25 °C, and molecular projected area of 130 $Å^2$ [13].

2.3. Physicochemical characterization of sawdust

The functional groups on the surface of NS were identified by Fourier Transform Infrared Spectroscopy (FTIR). The spectra were obtained using the technique of Attenuated Total Reflectance (ATR) coupled to an FTIR spectrometer, Cary 660 (Agilent, USA).

The concentrations of the active sites of the NS were determined by the acid-base titration method proposed by Boehm [38]. The total acidic and basic sites were neutralized with 0.01 M NaOH and HCl solutions, respectively. The total acidic sites included the carboxylic, phenolic and lactonic sites. Additionally, the carboxylic sites were neutralized with 0.01 M $NaHCO_3$ solution, and the lactonic sites with 0.01 M Na_2CO_3 solution. Lastly, the phenolic sites were estimated by subtracting the carboxylic and lactonic sites from the total acidic sites. The titration procedure can be described as follows. A portion of 0.1 g of the adsorbent and 45 mL of a neutralizing solution were added to a plastic bottle. After 5 d, a sample of the neutralizing solution (40 mL) was taken out and was titrated with 0.01 M NaOH or HCl solution, as required. The titration was carried out with an automatic titrator, model LD50 (Mettler-Toledo, USA).

The surface charge distribution and the pH of the point of zero charge (pH_{PZC}) for the NS were evaluated by a titration procedure described elsewhere [39]. Twenty neutralizing solutions of pH between 2 and 12 were prepared by adding volumes between 0.4 and 16 mL of 0.1 M NaOH or HCl solutions to 100 mL volumetric flasks and diluting up to the mark with a 0.1 M NaCl solution. A mass of 0.1 g of NS and 45 mL of neutralizing solution were added into a 50 mL polypropylene container, and nitrogen gas was bubbled for 2 min to prevent the formation of carbonates in the solution. The containers were covered and, twice a day, the solution into the container was mixed with an orbital Shaker at 300 rpm for 15 min. The above procedure was repeated without adding NS, and these experiments were designated as blanks. After 5 d, the final pH of the solutions was measured using a potentiometer. The potentiometric curves (volume of the neutralizing solution vs. pH_{final}) corresponding to solutions with NS and without NS were plotted. The intersection of both curves was the pH_{PZC} of NS. The surface charge distribution was estimated by the procedure and equations described by elsewhere [40].

The textural properties of the NS were determined by adsorption of N_2 at 77 K using a surface area and porosimeter analyzer, Model ASAP 2010 (Micromeritics, USA).

2.4. Determination of the MB concentration in water solutions

The concentration of MB in an aqueous solution was determined by a direct spectrophotometric method. The absorbance of a sample was measured in a double-beam UV/Vis spectrophotometer, UV2600 (Shimadzu, Japan), at a wavelength of 664.5 nm. Then, the concentration of MB in a sample was estimated using a calibration curve, concentration of the MB vs. absorbance. The calibration curve presented a linear behavior when the concentration of the MB ranged from 0.5 to 6 mg L^{-1}.

2.5. Procedure for obtaining experimental adsorption equilibrium data

A MB stock solution having a concentration of 1000 mg L^{-1} was prepared by adding 1 g of MB into a 1000 mL volumetric flask and dissolving with deionized water. Additionally, a solution with a constant ionic strength of 0.01 M and particular pH was fixed by mixing certain volumes of 0.01 M NaOH and HCl solutions. Then, a solution of a known initial concentration of MB and at a given pH was prepared by adding an aliquot of the MB stock solution to a

50 mL volumetric flask and diluting to the mark with a constant ionic strength solution. In some experiments, the ionic strength of the MB solution was 0.05 and 0.1 M, and these solutions were fixed using 0.05 or 0.1 M NaOH and HCl solutions.

The mass of MB adsorbed on NS was determined by the following procedure. A portion of 0.1 g of NS and 45 mL of a solution with an initial concentration of MB ranging from 50 to 400 mg L^{-1} and a particular pH were mixed in a batch adsorber (centrifuge vial of 50 mL). The adsorber was partially immersed in a thermostatic water bath, and the solution was mixed by placing the adsorber on top of an orbital shaker three times daily and for 15 min. In preliminary experiments, it was found that a period of four days was enough to attain equilibrium, and during this period, the pH of the adsorber solution was kept constant by adding few drops of 0.01 M NaOH or HCl solutions, as necessary. The total volume of solutions added to maintain pH constant was always less than 1 mL, and therefore, it was considered that the volume of the adsorber solution remained constant. The mass of MB adsorbed on NS was calculated by a mass balance of MB and the equation representing this mass balance is the following:

$$q_e = \frac{V(C_0 - C_e)}{m} \quad (1)$$

where C_0 and C_e are the initial and equilibrium concentrations of MB, respectively, mg L^{-1}; q_e is the mass of MB adsorbed per unit mass of NS, mg g^{-1}; V is the volume of the MB solution in the adsorber, L; and m is the mass of NS, g.

2.6. Experimental desorption equilibrium data

The experimental desorption equilibrium data of MB were obtained by first performing a biosorption run, as described above, and after reaching equilibrium, the desorption experiment started. The latter was carried out by removing the NS saturated with MB from the adsorption solution and then placing the NS saturated with MB in a 45 mL of a solution with a given pH and MB-free. Under these conditions, the MB is desorbed from NS to the solution, and equilibrium was again attained. If the adsorption is reversible, the desorption equilibrium data must be in the biosorption isotherm at the solution pH of the desorption solution.

The mass of MB that remained adsorbed was calculated from a mass balance of MB, which is shown below:

$$q_d = \frac{mq_0 - VC_e}{m} \quad (2)$$

where q_0 is the mass of MB biosorbed on the NS at the beginning of the desorption experiment, mg g^{-1}; and q_d is the mass of MB that remains biosorbed on the NS after desorption, mg g^{-1}.

2.7. Determination of the equivalents of H^+ exchanged

The equivalents of H^+ exchanged during the adsorption of MB were determined by the procedure suggested by Leyva-Ramos et al. [40]. A certain mass of NS and 45 mL of a MB-free solution at a given pH were added to a batch adsorber, and they were left in contact for few days. During this time, the solution pH was measured periodically using a pH-meter and was kept constant by adding few drops of 0.01 M of HCl and NaOH solutions, as necessary. The MB-free solution and the surface of NS were equilibrated when the pH did not vary over time. Soon afterward, an aliquot of a MB standard solution was added to the adsorber solution, and the initial concentration of MB in the adsorber solution was registered. It is important to point out that the pH of the MB standard solution must be the same as that of the adsorber solution. The solution and NS were left in contact for 4 d to reach equilibrium. The solution pH was no longer adjusted but was periodically measured using a pH-meter. After attaining equilibrium, the final solution pH was measured, and a sample was taken to determine the final concentration of MB at equilibrium.

The total milliequivalents of MB adsorbed by the different mechanism, Q_T, were estimated by the following equation:

$$Q_T = \frac{q_e}{EW_{MB}} \quad (3)$$

The milliequivalents of H^+ exchanged between the solution and the surface of NS were estimated as follows:

$$Q_{IEx} = \left(10^{-pH_{fn}} - 10^{-pH_{in}}\right)\frac{1000\,V}{m} \quad (4)$$

where EW_{MB} is the equivalent weight of MB, mg meq^{-1}; pH_{in} and pH_{fn} are the initial and final values of the solution pH before adding the aliquot of MB and after attaining equilibrium, respectively; Q_T represents the total milliequivalents of MB adsorbed, meq g^{-1}; and V is the final volume of the solution, L.

3. Results and discussion

3.1. Physicochemical characterization of natural sawdust

The concentrations of total acidic, phenolic, carboxylic and lactonic sites of NS were 0.12, 0.08, 0.004 and 0.03 meq g^{-1}, respectively, and the concentration of basic sites was 0.05 meq g^{-1}. Thus, the surface of NS has an acidic character since it has a higher concentration of acidic groups, mainly of the phenolic type. Phenolic groups are part of the molecular structure of lignin and cellulose, which are the main components of NS.

The distribution of the surface charge of NS is presented in Fig. 1 and the pH_{PZC} of NS is 4.25. This value confirms that the nature of the NS surface is acidic. The pH_{PZC} is defined as the pH value at which the density of surface charge of the biosorbent is neutral. The surface charge is positive when the pH of the solution is less than pH_{PZC} while it is negative for pH greater than the pH_{PZC}. This shows the close relationship existing between the surface functional groups of NS and its surface charge.

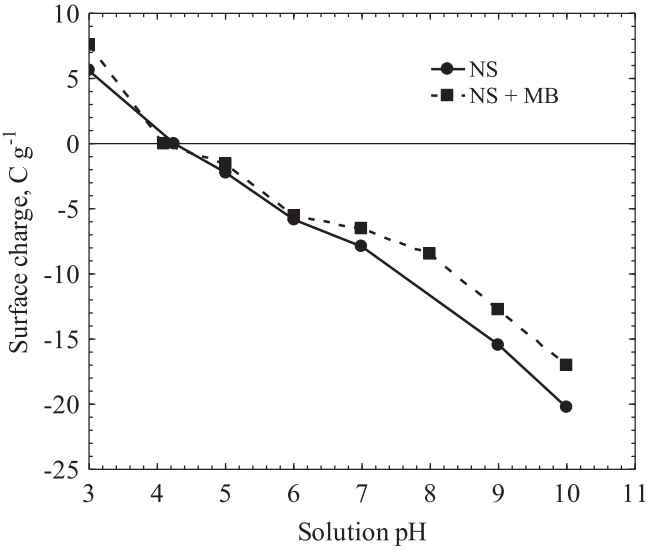

Fig. 1. Surface charge distribution of NS and NS saturated with MB (C_0 = 200 mg L^{-1}).

The pH_{PZC} of sawdust from Maple wood was determined to be 6 [41]. This result shows that Maple sawdust surface is slightly acidic in nature; however, the surface of NS from White Pine used in this study is more acidic. In a previous work, the pH_{PZC} of White Pine sawdust was found to be 3.65, which is closed to the value reported in this work [39].

Fig. 2a shows the infrared spectrum of NS in the range of 800–4000 cm^{-1} and there are two main regions of absorption. The bands observed in the range from 1500 to 1600 cm^{-1} can be associated with the vibrations of aromatic rings present in the structure of lignin. The pronounced band at 1000 cm^{-1} and the attenuated band at 1262 cm^{-1} correspond to the C–O group, which is characteristic of alcohols, esters and carboxylic acids, and all of them are present in the molecular structures of the principal components of NS. The carbonyl groups (C=O) exhibited a band at 1720 cm^{-1} and were present in various types of hemicellulose; its low intensity can be attributed to the low concentration of this substance in the NS. The band observed at 2916 cm^{-1} corresponded to the C–H group, owing to cellulose, hemicellulose and lignin. Lastly, the band at 3324 cm^{-1} was due to the O–H groups mostly present in the cellulose [42,43].

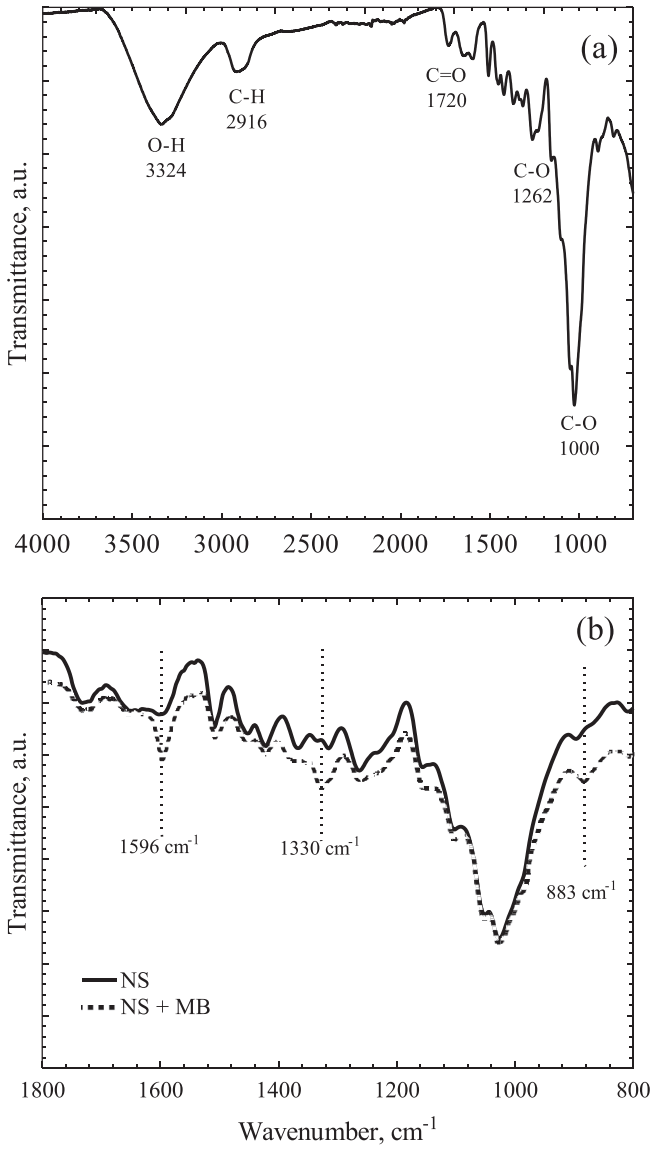

Fig. 2. FTIR spectra of (a) NS and (b) NS and NS loaded with MB (NS + MB) (T = 25 °C, pH = 10 and C_0 = 500 mg L^{-1}).

A zoom of the FTIR spectra of NS and NS saturated with MB (NS + MB) is depicted in Fig. 2b in the range from 800 to 1800 cm^{-1}. In this figure, it can be observed that both spectra are similar, but the spectrum of NS + MB exhibits two strong bands at 1596 cm^{-1} (–C=N– stretching in the poly heterocycles) and 1330 cm^{-1} (–C–N– stretching in amine groups) and one weak band at 883 cm^{-1} (–C–H out-of-plane bend in aromatic rings), which are characteristic of the MB [44]. This result corroborated the presence of MB in the NS + MB.

3.2. Textural properties of the natural sawdust

The surface area, mean pore diameter and total pore volume of NS were 0.4 $m^2\ g^{-1}$, 5.1 nm and $5.0 \times 10^{-4}\ cm^3\ g^{-1}$. In the technical literature, similar results have been reported for sawdust from meranti, oak, carob black, walnut, cherry and pine woods [11,45–47]. According to the classification of pores suggested by the IUPAC [48], the NS can be considered a mesoporous material since the average pore diameter was within 2 and 50 nm.

3.3. Adsorption isotherms of MB on natural sawdust

The biosorption equilibrium data of MB on NS at various experimental conditions were interpreted using the adsorption isotherm models of Freundlich, Langmuir, and Redlich–Petersen, which are represented by the following equations:

$$q = kC^{1/n} \tag{5}$$

$$q = \frac{q_m K_L C}{1 + K_L C} \tag{6}$$

$$q = \frac{aC}{1 + bC^{\beta}} \tag{7}$$

where a is a constant of the Redlich–Peterson isotherm, $L\ g^{-1}$; b is a constant of the Redlich–Peterson isotherm, $L^{\beta}\ mg^{-\beta}$; C is the concentration of MB at equilibrium, mg L^{-1}; k is a constant of the Freundlich isotherm, $mg^{1-1/n}L^{1/n}\ g^{-1}$; K_L is a constant of the Langmuir isotherm related to the heat of adsorption, L mg^{-1}; n is a constant of the Freundlich isotherm; q_m is the maximum mass of MB adsorbed on the NS, mg g^{-1}; and β is a constant of the Redlich–Peterson isotherm.

The parameters of the adsorption isotherms were estimated by a least-squares method based upon the optimization algorithm of Rosenbrock–Newton. The following objective function was minimized:

$$R = \sum \left(q_{exp} - q_{cal}\right)^2 = \text{Minimum} \tag{8}$$

In addition, the absolute average percentage deviation for each isotherm can be calculated from the following equation:

$$\%D = \left(\frac{1}{N}\sum_{i=1}^{N}\left|\frac{q_{exp} - q_{cal}}{q_{exp}}\right|\right) \times 100\% \tag{9}$$

The values of the parameters and %D for the Langmuir, Freundlich and Redlich–Petersen isotherms are reported in Table 1.

Table 1
Parameters of the isotherm models for the adsorption of MB on NS.

T (°C)	pH	Freundlich			Langmuir			Redlich–Peterson			
		k ($mg^{1-1/n}\ L^{1/n}\ g^{-1}$)	n	%D	q_m (mg g^{-1})	K_L (mg L^{-1})	%D	a (L g^{-1})	b ($L^{\beta}\ mg^{-\beta}$)	β	%D
25	3	20.1×10^2	2.40	1.4	23	0.020	7.9	13.5	6.69	0.58	1.8
25	4.25	12.7	6.11	10.6	32	0.084	7.5	2.4	0.07	1.03	7.7
25	7	19.1	7.89	6.0	38	0.26	2.1	11.8	0.35	0.98	2.0
25	10	30.8	4.87	10.7	85	0.22	5.7	22.1×10^2	0.32	0.96	5.7
15	10	18.4×10^2	3.70	5.0	77	0.071	7.0	21.8	0.86	0.79	4.7
35	10	30.6	4.31	11.8	102	0.24	15.5	35.8	0.93	0.82	10.9

Accordingly to the values of %D, the three models can effectively interpret the experimental data since the values they were less than 15.5% for all isotherm models. It was considered that the Redlich–Peterson isotherm provided the best fit to experimental data because the %D was the lowest for 4 of the 6 cases of experimental conditions (see Table 1). It is important to point out that the Redlich–Petersen isotherm is a general isotherm model that can be simplified into the Langmuir and Freundlich isotherms. Therefore, the adsorption equilibrium of MB on NS was represented by the Redlich–Petersen isotherm.

At the different experimental conditions, the adsorption capacities could not be compared using the maximum adsorption capacity q_m of the Langmuir isotherm because, in some cases, the Langmuir isotherm did not fit reasonably well the experimental data. The adsorption capacities were compared by estimating the uptake of MB adsorbed at an equilibrium concentration of 300 mg L^{-1}. This uptake was designated as Q_{300} and was calculated using the Redlich–Peterson isotherm. The concentration of 300 mg L^{-1} was chosen because this value represented the maximum concentration where there were experimental uptake data for all conditions.

3.4. Effect of pH on the adsorption capacity

The adsorption capacity of a biomaterial towards MB is highly dependent on the solution pH since it affects the speciation of the MB in solution and the surface charge distribution of the biomaterial. In other words, the pH can influence the electrostatic interactions of attractive or repulsive character between the species of MB in the solution and the surface of the NS.

The MB can be present in aqueous solution as the cationic species (MB^+) and undissociated molecules (MB°). The speciation diagram of the MB is shown in Fig. 3. As seen in this figure, the MB° species predominates (86%) at pH = 3, both MB° (50%) and MB^+ (50%) species coexist at pH = pK_a = 3.8, and MB^+ is practically the only species present at pH > 6.

The effect of pH on the adsorption capacity of NS towards MB in aqueous solution was investigated by obtaining the adsorption isotherms at pH of 3, 4.25, 7 and 10. The pH of 4.25 was selected since this pH corresponds to pH_{PZC}. Fig. 4 illustrates the effect of pH on the adsorption capacity, and it can be observed that the capacity of NS for biosorbing MB increased considerably when the solution pH was raised. The values of the adsorption capacity Q_{300} were 22, 31, 38 and 87 mg g^{-1} at pH 3, 4.25, 7 and 10, respectively. Hence, the adsorption capacity was enhanced 1.4, 1.8 and 4.0 times while the solution pH was increased from 3 to 4.25, 3 to 7 and 3 to 10, correspondingly.

The low adsorption capacity of NS at pH = 3 can be explained by the fact that the MB is mainly found as a undissociated species, MB°, (≈ 86%) at this pH (see Fig. 3) and the NS surface is positively charged at pH values < pH_{PZC} = 4.25. Therefore, the adsorption of MB was disfavored by the electrostatic repulsion between the MB^+ (≈ 14%) and the surface of the NS. This result suggests the MB was predominantly adsorbed as MB° on NS at pH = 3.

The gradual increase in the adsorption capacity for pH > pH_{PZC} was mainly due to that the cationic MB^+ was the predominant species of MB while the charge of NS surface became negative. Additionally, the negative charge of the surface increased by raising the solution pH. The electrostatic attraction between the MB^+ and the negative surface of NS favored the adsorption capacity of NS.

To corroborate the influence of the electrostatic attractions on the adsorption capacity, the surface charge of the NS saturated with

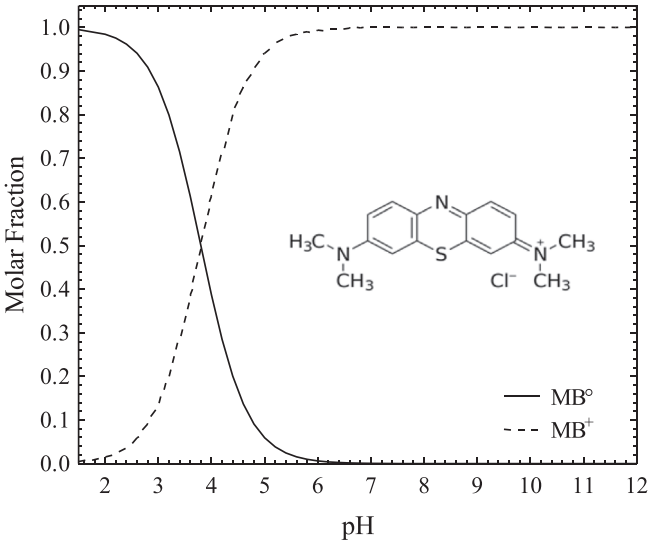

Fig. 3. Speciation diagram of the MB (C_0 = 1000 mg L^{-1}) and molecular structure of the MB.

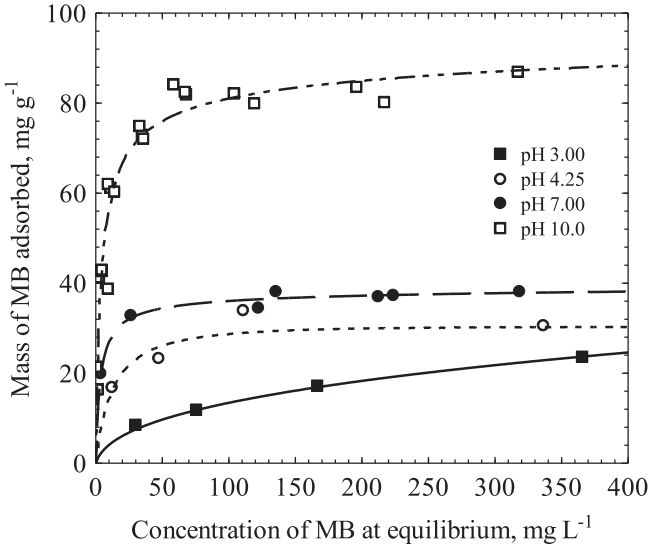

Fig. 4. Effect of the solution pH on the adsorption isotherm of MB on NS at T = 25 °C. The lines represent the Redlich–Peterson adsorption isotherm.

MB was measured and compared to that of NS. The surface charge of the NS saturated with MB was determined by performing adsorption runs using the experimental conditions for evaluating the surface charge distribution and an initial MB concentration of 200 mg g^{-1} and pH of 3, 4.25, 7 and 10. After attaining equilibrium, the mass of MB adsorbed was determined and then, the surface charge of NS saturated with MB was evaluated as describe in a previous section. The surface charge of NS saturated with MB is graphed in Fig. 1, and it can be noticed that the negative charge of the NS saturated with MB was lessened comparing with that of the NS. This result reveals that the MB^+ adsorbed on the NS surface and balanced the negative charge of NS. Hence, one of the adsorption mechanisms of MB is the electrostatic attraction.

At pH = pH_{PZC}, MB was adsorbed on NS even though the surface charge was neutral, indicating that MB was adsorbed by other mechanisms than electrostatic attraction. At pH < pH_{PZC}, the positive charge of the NS saturated with MB was increased while MB was being adsorbed. The species of MB present at pH = 3 are MB° (86%) and MB^+ (14%) so that part of the MB^+ was adsorbed increasing the positive charge of the NS surface, but the adsorption of MB^+ was due to a mechanism different from the electrostatic attraction.

3.5. Effect of temperature in adsorption capacity

The biosorption isotherm is affected by the temperature because it represents the thermodynamic equilibrium between MB biosorbed on the surface of NS and MB in water solution. The effect of temperature on the capacity of the NS for adsorbing MB was analyzed by determining the biosorption isotherms of MB on NS from aqueous solution at the temperatures of 15, 25 and 35 °C and pH = 10 (Fig. 5). The latter was selected because the maximum adsorption capacity was observed at this pH. The values of the adsorption capacity Q_{300} were 83, 87 and 108 mg g^{-1} at the temperatures of 15, 25 and 35 °C, correspondingly. This trend represented an increase in the adsorption capacity of 1.05 and 1.3 times, when the temperature was elevated from 15 to 25 °C and 25 to 35 °C, respectively. However, for concentrations of MB at equilibrium less than 70 mg L^{-1}, the adsorption capacity of NS did not vary with temperature, when the temperature was increased from 25 to 35 °C. This unusual behavior can be attributed to the adsorption mechanism of MB being dependent on the temperature and mass of MB adsorbed.

The heat of adsorption of MB onto NS was estimated by the van't Hoff equation [49], which is shown below in its linearized form:

$$\text{Ln } K_L = -\frac{\Delta H_{Ad}}{R}\frac{1}{T} + \text{Ln } K_{L0} \quad (10)$$

where ΔH_{ads} is the heat of biosorption, J mol^{-1}; T is the temperature of the solution, K; R is the ideal gas law constant, 8.31 J mol^{-1} K^{-1}; and K_{L0} is the pre-exponential factor, L mg^{-1}. The experimental values of K (Table 1) were fitted to Eq. (10) and the ΔH_{ads} was estimated to be 46 kJ mol^{-1}, indicating that the biosorption of MB on NS was an endothermic process. In the endothermic processes, the adsorption equilibrium can be enhanced by increasing the temperature. This explains why the adsorption capacity increased with temperature. It is important to point out that the ΔH_{ads} was closed to 42 kJ mol^{-1}, corresponding to a chemical reaction or interaction [50]. Thus, a part of MB was chemisorbed on NS.

3.6. Effect of ionic strength

The effect of the ionic strength of the solution on the adsorption capacity of NS was studied to examine the importance of the electrostatic interactions during the biosorption process. Schiewer and Volesky [51] and Rivera-Utrilla and Sánchez-Polo [52] reported that the presence of electrolytes can influence the strength of electrostatic interactions between the adsorbate and the biosorbent surface due to a screening effect.

Fig. 6 shows the uptake of MB biosorbed on NS at an initial MB concentration of 300 mg L^{-1}, pH of 3, 7 and 10, and ionic strengths of 0.01, 0.05 and 0.10 M. The results graphed in this figure revealed that the mass of MB adsorbed was drastically reduced by increasing the ionic strength of the solution, corroborating that the electrostatic attraction played a significant role in the adsorption of MB on NS. Han et al. [53] found similar trend for the adsorption capacity of chaff towards MB. The reduction of the mass of MB adsorbed caused by increasing the ionic strength was much more significant for pH = 10 than pH = 3. This trend was attributed to that the electrostatic attractions were more important at the pH = 10. At an ionic strength of 0.01 M, the adsorption capacity increased drastically by raising the solution pH, whereas, at an ionic strength of 0.1 M, the adsorption capacity was almost independent on the solution pH. The adsorption of Na^+ cations on the surface of NS

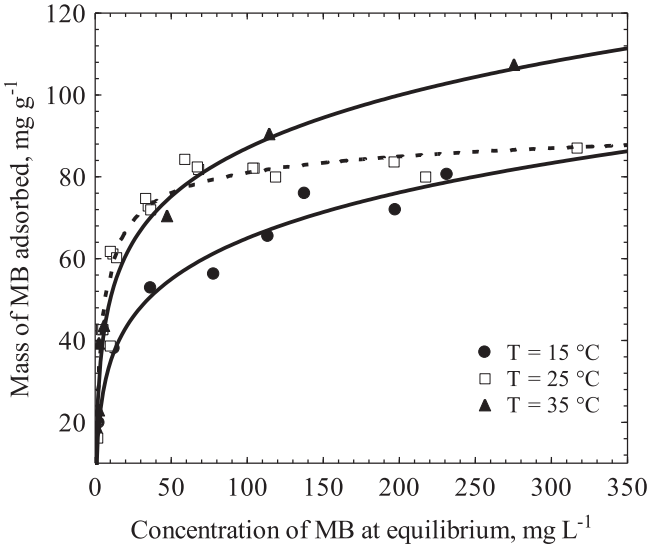

Fig. 5. Effect of temperature on the adsorption isotherm of MB on NS at pH = 10. The lines represent the Redlich–Peterson isotherm.

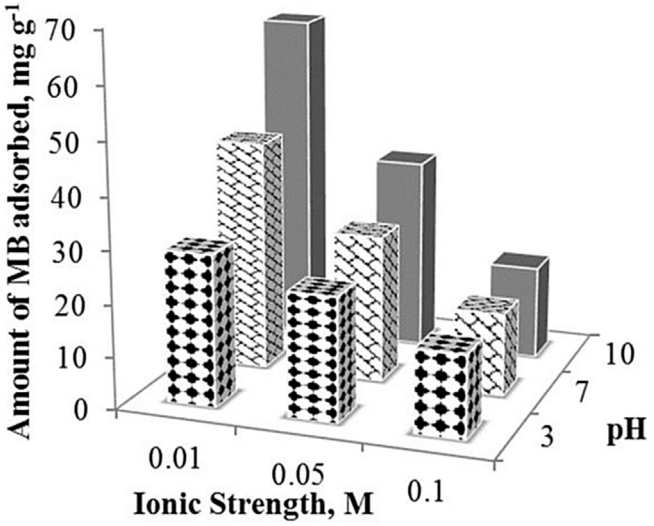

Fig. 6. Effect of the ionic strength on the adsorption capacity of NS towards MB at pH of 3, 7 and 10, T = 25 °C and C_0 = 300 mg L^{-1}.

balanced or shielded the negative charge of the NS surface so that the electrostatic attraction between the MB^+ and the surface of NS was decreased causing a reduction in the adsorption capacity of NS. This behavior is known as the screening effect.

3.7. Reversibility of the biosorption of MB

The purpose of studying the reversibility of the biosorption process was to obtain additional information on the nature of the interactions occurring in the adsorption of MB on the surface of NS. If the biosorption was reversible, the biosorption mechanism would be due to weak interactions (electrostatic or dispersive). On the other hand, if the adsorption of MB was irreversible, then the interaction between MB and the surface of NS would be strong, and part of MB can be chemisorbed on NS.

The reversibility of the biosorption of MB on NS was investigated by carrying out adsorption experiments at pH = 10, and then desorption experiments at pH 10 or 3. The adsorption isotherms and the experimental adsorption and desorption equilibrium data of MB on NS are plotted in Fig. 7a for adsorption and desorption at pH = 10, and in Fig. 7b for the adsorption at pH = 10 and desorption at pH = 3. The adsorption data were designated as *Ads* and desorption data as *Des*. Fig. 7a shows that desorption equilibrium data at pH = 10 are on the adsorption isotherm at the same pH when the concentration of MB at equilibrium is less than 5 mg L^{-1}, indicating that the biosorption was reversible. However, the biosorption was irreversible for concentrations of MB at equilibrium greater than 5 mg L^{-1}. This behavior showed that the MB was mainly adsorbed by a reversible mechanism for MB concentrations at equilibrium less than 5 mg L^{-1}, whereas for MB concentrations greater than 5 mg L^{-1}, the biosorption probably occurred by two mechanisms. One of the mechanisms was reversible, i.e., electrostatic attraction and the other was irreversible, i.e., chemisorption.

The desorption equilibrium data of MB at pH = 3 shown in Fig. 7b indicated the data were not on the biosorption isotherm at pH = 3, revealing that the biosorption was not reversible at this pH. A significant amount of MB was desorbed when the desorption step was carried out at pH = 3. These results suggest that one of the biosorption mechanisms of MB is chemisorption or a chemical interaction. Furthermore, these results indicate that the sawdust can be partially regenerated by desorbing the MB from the sawdust saturated with MB using a water solution at pH = 3.

3.8. Biosorption mechanism of MB

The results of the effect of the pH on the biosorption equilibrium of MB showed that the adsorption capacity of the NS towards MB increased drastically by raising the pH. At pH values of 7 and 10, the dominant species was the cationic MB^+ and was attracted electrostatically by the negatively charged surface of NS, and the electrostatic attraction was stronger when the solution pH was increased. However, the electrostatic attraction was not the only adsorption mechanism of MB since the NS presented a reasonably good adsorption capacity towards MB at pH = 3, even though the electrostatic interactions did not favor the adsorption. At pH = 3, the molecule of MB was as the neutral species MB° and the surface of NS was positively charged. Under these experimental conditions, the adsorption of MB can be attributed, in part, to π–π dispersive interactions between the π-electrons of the aromatic rings of the MB and the π-electrons from the aromatic rings of lignin [52]. Moreover, the reversibility experiments showed that adsorption of MB was not reversible, indicating that the adsorption mechanism of MB on NS was due to weak as well as strong interactions between the surface of NS and MB.

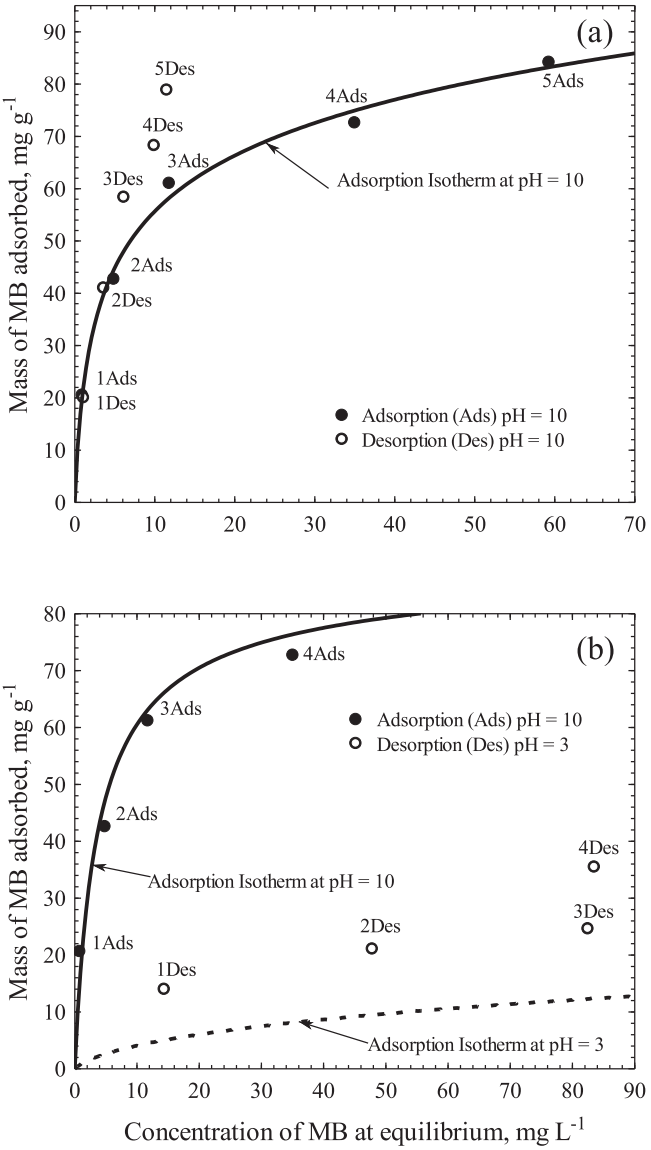

Fig. 7. Adsorption–desorption isotherms of MB on NS. Adsorption at pH = 10 and desorption at pH = 10 (a). Adsorption at pH = 10 and desorption at pH = 3 (b). T = 25 °C. The lines represent the Redlich–Peterson isotherm.

The contribution of ion exchange in the adsorption of MB was evaluated by determining the equivalents of protons displaced from the NS during the adsorption of MB. The milliequivalents of H^+ exchanged from the surface of NS to the solution during biosorption, Q_{IEx}, were assumed to be equal to the uptake of MB^+ adsorbed on the surface of NS by ion exchange. The uptake of MB adsorbed by other mechanisms (Q_{OM}) was the difference between the total uptake of MB adsorbed (Q_T) and the uptake of MB adsorbed by ion exchange (Q_{IEx}). Electrostatic attractions, dispersive interactions and chemisorption are included in other mechanisms.

Table 2 shows the experimental data for the milliequivalents of H^+ exchanged from the surface of the NS during the adsorption of MB, and it can be observed that the amount of MB adsorbed by ion exchange can be considered negligible compared to the contribution of other mechanisms. Moreover, Q_{IEx} presented negative values at $pH_{in} \approx 3.0$ indicating that the protons were exchanged from the solution to the surface of NS in the same direction as MB

Table 2
Experimental data for proton displacement during the adsorption of MB from aqueous solution on NS. T = 25 °C.

Exp. No.	pH_{in}	pH_{fn}	$Q_T \times 10^2$ (meq g^{-1})	$Q_{IEx} \times 10^{a*}$ (meq g^{-1})	$Q_{OM} \times 10^2$ (meq g^{-1})	% IEx	% OM
1AM	2.90	2.92	1.2	−2.5	3.7	N.A.	N.A.
2AM	3.09	3.09	1.4	0.0	1.4	N.A.	N.A.
3AM	2.91	2.99	2.0	−9.3	11.3	N.A.	N.A.
4AM	3.04	3.23	1.9	−14.5	16.4	N.A.	N.A.
5AM	2.97	3.16	1.7	−17.1	18.8	N.A.	N.A.
1BM	7.04	6.71	5.0	4.6	5.0	0.09	99.91
2BM	7.05	6.86	8.0	2.2	8.0	0.03	99.97
3BM	6.97	6.84	8.0	1.7	8.0	0.02	99.98
4BM	7.05	6.75	6.6	4.0	6.6	0.06	99.94
5BM	7.06	6.66	10.3	5.9	10.3	0.06	99.94
1CM	10.0	9.40	6.0	1.3	6.0	0.00	100.0
2CM	9.92	9.46	10.3	1.0	10.3	0.00	100.0
3CM	10.2	8.84	13.3	6.12	13.3	0.00	100.0
4CM	10.1	8.92	16.3	4.99	16.3	0.00	100.0
5CM	10.1	8.02	13.3	42.3	13.3	0.00	100.0

*The value of *a* was 2, 5 and 7 for the experiments designated as AM, BM and CM, respectively. N.A. = Not Applicable.

was being adsorbed. In other words, the cationic MB^+ competed with H^+ for the active sites of NS. Furthermore, the contribution percentage by other mechanisms (%OM) was estimated by the following equation:

$$\%OM = \frac{Q_{OM}}{Q_T} \times 100\% \quad (11)$$

The values of %OM are also given in Table 2 and are practically 100% for pH values of 7 and 10. This result corroborated that MB was primarily adsorbed on NS by mechanisms such as electrostatic attraction (particularly at basic pH values), dispersive interactions and chemisorption.

4. Conclusions

It was found that the surface of the NS was acidic because of the phenolic groups from the lignocellulosic materials. The acidic nature of NS was also corroborated by its pH of the point zero charge of 4.25 and the infrared spectrum of the NS demonstrated the presence of the phenolic groups in the NS.

The experimental biosorption equilibrium data of the MB on NS were interpreted using the isotherm models of Langmuir, Freundlich and Redlich–Peterson. In general, the Redlich–Peterson isotherm provided the best fit since this isotherm presented the lowest absolute percentage average deviation.

The uptake of MB adsorbed on NS was highly dependent on the solution pH. The capacity of NS for biosorbing MB was increased 1.7, 2.0 and 4.6 times when the pH was raised from 3 to 4.25, 3 to 7 and 3 to 10, respectively. This enhancement was due to the increase in the electrostatic attractions between the cationic MB^+ in the solution and the negatively charged surface of NS.

The effect of temperature revealed that adsorption of MB on NS was an endothermic process, and its heat of adsorption was 46 kJ mol^{-1}. For this reason, the adsorption capacity of NS was favored by increasing the temperature.

The main adsorption mechanism of MB on the NS from water solutions was the electrostatic attraction, especially at basic pH. This result was confirmed by noticing that the uptake of MB adsorbed increased by raising the pH of the solution and by reducing the ionic strength of the solution. Both effects can be attributed to the electrostatic attraction between the cationic MB^+ and the negatively charged surface of NS. The reversibility studies demonstrated that the adsorption was not reversible. Hence, chemisorption was another mechanism contributing to the biosorption of MB, although to a lesser extent.

Acknowledgements

This work was funded by the Consejo Nacional de Ciencia y Tecnologia, CONACyT, Mexico, through grants: CONAFOR-2010-C02-148302 and CB-2012-02-182779.

References

[1] Bhatnagar A, Jain AK. A comparative study with different industrial wastes as adsorbents for removal of cationic dyes from water. J Colloid Interf Sci 2005;281:49–55.
[2] Royer B, Cardoso NF, Lima EC, Vaghetti JCP, Simon NM, Calvete T, et al. Applications of Brazilian pine-fruit shell in natural and carbonized forms as adsorbents to removal of Methylene Blue from aqueous solutions. Kinetic and equilibrium study. J Hazard Mater 2009;169:1213–22.
[3] Height MJ, Pratsinis SE, Mekasuwandumrong O, Praserthdam P. Ag-ZnO catalysts for UV-photodegradation of Methylene Blue. Appl Catal B-Environ 2001;63:305–12.
[4] Ji F, Li C, Zhang J, Deng L. Heterogeneous photo-Fenton decolorization of Methylene Blue over $LiFe(WO_4)_2$ catalyst. J Hazard Mater 2011;186:1979–84.
[5] Liang X, Zhong Y, Zhu S, Ma L, Yuan P, Zhu J, et al. The contribution of vanadium and titanium on improving Methylene Blue decolorization through heterogeneous UV-Fenton reaction catalyzed by their co-doped magnetite. J Hazard Mater 2012;199–200:247–54.
[6] Mahmoodi NM, Arami M, Zhang J. Preparation and photocatalytic activity of immobilized composite photocatalyst (titania nanoparticle/activated carbon). J Alloy Compd 2011;509:4754–64.
[7] Torres-Luna JR, Ocampo-Pérez R, Sánchez-Polo M, Rivera-Utrilla J, Velo-Gala I, Bernal-Jácome LA. Role of $HO^•$ and $SO_4^•$ radicals on the photodegradation of remazol red in aqueous solution. Chem Eng J 2013;223:155–63.
[8] Xiong L, Sun W, Yang Y, Chen C, Ni J. Heterogeneous photocatalysis of Methylene Blue over titanate nanotubes: effect of adsorption. J Colloid Interf Sci 2011;356:211–6.
[9] Zhang Q, Li C, Li T. Rapid photocatalytic decolorization of Methylene Blue using high photon flux $UV/TiO_2/H_2O_2$. Chem Eng J 2013;217:407–13.
[10] Houas A, Lachheb H, Ksibi M, Elaloui E, Guillard C, Herrmann JL. Photocatalytic degradation pathway of Methylene Blue in water. Appl Catal B-Environ 2001;31:145–57.
[11] Ferrero F. Dye removal by low cost adsorbents: hazelnut shells in comparison with wood sawdust. J Hazard Mater 2007;142:144–52.
[12] Hamdaoui O. Batch study of liquid-phase adsorption of Methylene Blue using cedar sawdust and crushed brick. J Hazard Mater 2006;135:264–73.
[13] Ocampo-Pérez R, Leyva-Ramos R, Sánchez-Polo M, Rivera-Utrilla J. Role of pore volume and surface diffusion in the adsorption of aromatic compounds on activated carbon. Adsorption 2013;19:945–57.
[14] Ofomaja AE. Kinetic study and sorption mechanism of Methylene Blue and methyl violet onto mansonia (*Mansonia altissima*) wood sawdust. Chem Eng J 2008;143:85–95.
[15] Yao Y, Xu F, Chen M, Xu Z, Zhu Z. Adsorption behavior of Methylene Blue on carbon nanotubes. Bioresour Technol 2010;101:3040–6.
[16] Asfaram A, Ghaedi M, Hajati S, Goudarzi A. Synthesis of magnetic γ-Fe_2O_3-based nanomaterial for ultrasonic assisted dyes adsorption: modeling and optimization. Ultrason Sonochem 2016;32:418–31.
[17] Chen Z, Fu J, Wang M, Zhang J, Xu Q. Adsorption of cationic dye (Methylene Blue) from aqueous solution using poly(cyclotriphosphazene-co-4,4-sulfonyldiphenol) nanospheres. Appl Surf Sci 2014;289:495–501.

[18] Chiu KL, Ng DHL. Synthesis and characterization of cotton-made activated carbon fiber and its adsorption of Methylene Blue in water treatment. Biomass Bioenerg 2012;46:102–10.
[19] Gatica JM, Gómez DM, Harti S, Vidal H. Clay honeycomb monoliths for water purification: modulating Methylene Blue adsorption through controlled activation via natural coal templating. Appl Surf Sci 2013;277:242–8.
[20] Rida K, Bouraoui S, Hadnine S. Adsorption of Methylene Blue from aqueous solution by kaolin and zeolite. Appl Clay Sci 2013;83–84:99–105.
[21] Wu Z, Joo H, Lee K. Kinetics and thermodynamics of the organic dye adsorption on the mesoporous hybrid xerogel. Chem Eng J 2005;112:227–36.
[22] Yan H, Tao X, Yang Z, Li K, Yang H, Li A, et al. Effects of the oxidation degree of graphene oxide on the adsorption of Methylene Blue. J Hazard Mater 2014;268:191–8.
[23] Asfaram A, Ghaedi M, Hajati S, Rezaeinejad M, Goudarzi A, Purkait MK. Rapid removal of auramine-O and Methylene Blue by ZnS: Cu nanoparticles loaded on activated carbon: a response surface methodology approach. J Taiwan Inst Chem Eng 2015;53:80–91.
[24] Radovic LR, Moreno-Castilla C, Rivera-Utrilla J. Carbon materials as adsorbents in aqueous solutions. In: Radovic LR, editor. Chemistry and Physics of Carbon. New York: Marcel Dekker; 2001. p. 227–405.
[25] Rodríguez-Reinoso F, Marsh H, Heintz EA. Introduction to Carbon Technologies. 1st ed. Alicante, Spain: Publicaciones de la Universidad de Alicante; 1997.
[26] Annadurai G, Juang R, Lee D. Use of cellulose-based wastes for adsorption of dyes from aqueous solutions. J Hazard Mater 2002;92:263–74.
[27] Demarchi CA, Debrassi A, Rodrigues CA. The use of Jatoba bark for removal of cationic dyes. Color Technol 2012;128:208–17.
[28] Filho NC, Venancio EC, Barriquello MF, Hechenleitner AAW, Pineda EAG. Methylene Blue adsorption onto modified lignin from sugar cane bagasse. Eclet Quim 2007;32:63–70.
[29] Han X, Niu X, Ma X. Adsorption characteristics of Methylene Blue on poplar leaf in batch mode: equilibrium, kinetics and thermodynamics. Korean J Chem Eng 2012;29:494–502.
[30] McKay G, Porter JF, Prasad GR. The removal of dye colours from aqueous solutions by adsorption on low-cost materials. Water Air Soil Pollut 1999;114:423–38.
[31] Pavan FA, Gushikem Y, Mazzocato AC, Dias SLP, Lima EC. Statistical design of experiments as a tool for optimizing the batch conditions to Methylene Blue biosorption on yellow passion fruit and mandarin peels. Dyes Pigments 2007;72:256–66.
[32] Rosas-Castor JM, Garza-González MT, García-Reyes RB, Soto-Regalado E, Cerino-Córdova FJ, García-Gonzalez A, et al. Methylene Blue biosorption by pericarp of corn, alfalfa, and agave bagasse wastes. Environ Technol 2014;35:1077–90.
[33] Sharma P, Kaur H, Sharma M, Sahore V. A review on applicability of naturally available adsorbents for the removal of hazardous dyes from aqueous waste. Environ Monit Assess 2011;183:151–95.
[34] Malmström K, Savolainen J, Terho EO. Allergic alveolitis from pine sawdust. Allergy 1999;54:526–33.
[35] Parab H, Sudersanan M, Shenoy N, Pathare T, Vaze B. Use of agro-industrial wastes for removal of basic dyes from aqueous solutions. Clean-Soil Air Water 2009;37:963–9.
[36] Batzias FA, Sidiras DK. Simulation of dye adsorption by beech sawdust as affected by pH. J Hazard Mater 2007;141:668–79.
[37] Park AD. Environmental influences on post-harvest natural regeneration in Mexican pine-oak forests. For Ecol Manag 2001;144:213–28.
[38] Boehm HP. Some aspects of the surface chemistry of carbon blacks and other carbons. Carbon 1994;32:759–69.
[39] Salazar-Rábago JJ, Leyva-Ramos R. Novel biosorbent with high adsorption capacity prepared by chemical modification of white pine (*Pinus durangensis*) sawdust. Adsorption of Pb(II) from aqueous solutions. J Environ Manag 2016;169:303–12.
[40] Leyva-Ramos R, Berber-Mendoza MS, Salazar-Rabago J, Guerrero-Coronado RM, Mendoza-Barron J. Adsorption of lead(II) from aqueous solution onto several types of activated carbon fibers. Adsorption 2011;17:515–26.
[41] Yu LJ, Shukla SS, Dorris KL, Shukla A, Margrave JL. Adsorption of chromium from aqueous solutions by maple sawdust. J Hazard Mater 2003;B100:53–63.
[42] Reddy N, Yang Y. Structure and properties of high quality natural cellulose fiber from cornstalks. Polymer 2005;46:5494–500.
[43] Wade LG. Organic Chemistry. 5th ed. Upper Saddle River, NJ: Prentice Hall; 2003.
[44] Olivella MA, Fiol N, de la Torre F, Poch J, Villaescusa I. A mechanistic approach to Methylene Blue sorption on two vegetable wastes: cork bark and grape stalks. Bioresources 2012;73:3340–54.
[45] Rafatullah M, Sulaiman O, Hashim R, Ahmad A. Adsorption of copper (II), chromium (III), nickel (II) and lead (II) ions from aqueous solutions by meranti sawdust. J Hazard Mater 2009;170:969–77.
[46] Šćiban M, Klasnja M, Skrbic B. Modified hardwood sawdust as adsorbent of heavy metal ions from water. Wood Sci Technol 2006;40:217–27.
[47] Šćiban M, Radetic B, Kevresan Z, Klasnja M. Adsorption of heavy metals from electroplating wastewater by wood sawdust. Bioresour Technol 2007;98:402–9.
[48] Rouquerol J, Rouquerol F, Sing KSW, Llewellyn P, Maurin G. Adsorption by Powders and Porous Solids: Principles, Methodology and Applications. 2nd ed. London, UK: Academic Press; 2014.
[49] Do DD. Adsorption Analysis: Equilibria and Kinetics. 1st ed. London, UK: Imperial College Press; 1998.
[50] Froment GF, Bischoff KB. Chemical Reactor Analysis and Design. 2nd ed. Singapore: John Wiley & Sons; 1990.
[51] Schiewer S, Volesky B. Ionic strength and electrostatic effects in biosorption of divalent metal ions and protons. Environ Sci Technol 1997;31:2478–85.
[52] Rivera-Utrilla J, Sánchez-Polo M. The role of dispersive and electrostatic interactions in the aqueous phase adsorption of naphthalenesulphonic acids on ozone-treated activated carbons. Carbon 2002;40:2685–91.
[53] Han R, Wang Y, Han P, Shi J, Yang J, Lu Y. Removal of Methylene Blue from aqueous solution by chaff in batch mode. J Hazard Mater 2006;B137:550–7.